Light- and STM-Tip-Induced Formation of One-Dimensional and Two-Dimensional Organic Nanostructures†

ARTICLE *in* LANGMUIR · APRIL 2003

Impact Factor: 4.46 · DOI: 10.1021/la027051p · Source: OAI

Light- and STM-Tip-Induced Formation of One-Dimensional and Two-Dimensional Organic Nanostructures†

Atsushi Miura,‡ Steven De Feyter,*,‡ Mohamed M. S. Abdel-Mottaleb,‡ André Gesquière,‡ Petrus C. M. Grim,‡ Georg Moessner,§ Michel Sieffert,§ Markus Klapper,§ Klaus Müllen,*,§ and Frans C. De Schryver*,‡

Department of Chemistry, Laboratory of Molecular Dynamics and Spectroscopy, University of Leuven (KULeuven), Celestijnenlaan 200-F, 3001 Leuven, Belgium, and Max-Planck-Institut for Polymer Research, Ackermannweg 10, D-55128 Mainz, Germany

Received December 20, 2002. In Final Form: March 4, 2003

The light-induced and tip-induced polymerization of two diacetylene derivatives has been investigated at the air/solid interface by scanning tunneling microscopy (STM). One molecule is an isophthalic acid derivative with one diacetylene group, while the other one, a terephthalic acid derivative, contains two diacetylene functions. The design of the molecules (symmetry, presence of alkyl chains and hydrogen bonding moieties) leads to the formation of highly ordered two-dimensional patterns where the diacetylene groups stack in an optimal fashion. Both diacetylene derivatives can be polymerized by UV light irradiation, and locally the polymerization can be initiated and controlled by the STM tip. In addition to the formation of one-dimensional organic structures, it was possible to create two-dimensional organic nanostructures.

1. Introduction

The quest for increasingly smaller electronic devices has stimulated the field of molecular electronics. In the field of molecular electronics, semiconductors such as silicon-based transistors are replaced by molecular assemblies, which are functioning in a way similar to that of solid-state capacitors, diodes, and transistors. Molecular electronic nanodevices such as single-electron transistors, ultrahigh-density memory devices, nanocapacitors, and molecular rectifiers have been made.[1−4] Nevertheless, the application of molecular electronic devices is still in its infancy because of the difficulties in controlling the growth of organic structures in the nanometer regime and in connecting molecules to one another. New ways for the precise control and creation of nanoscale organic structures have to be established. In addition, the molecular device should have uniform and well-defined properties resulting from a well-ordered and highly stable molecular arrangement.

One possibility is the formation of highly ordered two-dimensional templates which by postprocessing can give rise to the desired nanostructures. Self-assembly at surfaces is a very efficient tool to construct highly ordered thin films. The formation of self-assembled monolayers by chemisorption of, for example, thiol derivatives on gold is a popular approach.[5,6] Another approach, which is based on the physisorption of molecules on a substrate, has also great potential.[7] In contrast to the chemisorbed systems where the molecular backbone is approximately perpendicular to the surface, the formation of two-dimensional adlayers with the molecules lying flat on the surface is easily achieved. The main advantage of the latter approach is that the functional groups are easily accessible for posttreatment.

One way to study the material and/or ordered structure properties with very high resolution is scanning tunneling microscopy (STM). In the past decade, spontaneously organized monolayers of organic compounds formed at the liquid/substrate interface have been extensively studied with STM.[7−11] Not only does STM allow the observation of two-dimensional (2D) molecular organization, but also it offers opportunities to investigate dynamic[12−14] and chemical[15−20] phenomena at surfaces with high spatial resolution.

Diacetylene compounds are known to polymerize topochemically by appropriate stimuli such as UV irradiation and heating.[21,22] In a previous paper, we observed the

* To whom correspondence should be addressed. E-mail: muellen@mpip-mainz.mpg.de, Frans.DeSchryver@chem.kuleuven.ac.be, Steven.DeFeyter@chem.kuleuven.ac.be.

† Part of the *Langmuir* special issue dedicated to David O'Brien.

‡ University of Leuven (KULeuven).

§ Max-Planck-Institut for Polymer Research.

(1) *Molecular Electronics*; Jortner, J., Ratner, M., Eds.; IUPAC Chemistry for the 21st Century Monographs; Blackwell Science: Oxford, 1997.

(2) *Molecular Electronics*; Ashwell, G. J., Ed.; Wiley: New York, 1992.

(3) Joachim, C.; Gimzewski, J. K.; Aviram, A. *Nature* **2000**, *408*, 541.

(4) Duan, X.; Huang, Y.; Cui, Y.; Wang, J.; Lieber, C. M. *Nature* **2001**, *409*, 66.

(5) Ulman, A. *Chem. Rev.* **1996**, *96*, 1533−1554 and references therein.

(6) Kim, T.; Ye, Q.; Sun, L.; Chan, K. C.; Crooks, R. M. *Langmuir* **1996**, *12*, 6065.

(7) Rabe, J. P.; Buchholz, S. *Science* **1991**, *253*, 424.

(8) McGonical, G. C.; Bernhardt, R. H.; Thomson, D. *J. Appl. Phys. Lett.* **1990**, *57*, 28.

(9) Frommer, J. *Angew. Chem., Int. Ed. Engl.* **1992**, *31*, 1298.

(10) Cyr, D. M.; Venkataraman, B. G.; Flynn, W. *Chem. Mater.* **1996**, *8*, 1600.

(11) De Feyter, S.; Gesquière, A.; Abdel-Mottaleb, M. M.; Grim, P. C. M.; Sieffert, M.; Meiners, C.; Valiyaveettil, S.; Müllen, K.; De Schryver, F. C. *Acc. Chem. Res.* **2000**, *33*, 520.

(12) Gesquière, A.; Abdel-Mottaleb, M. M.; De Feyter, S.; De Schryver, F. C.; Sieffert, M.; Müllen, K.; Calderone, A.; Lazzaroni, R.; Bredas, J. L. *Chem.—Eur. J.* **2000**, *6*, 3739.

(13) Padowitz, D. F.; Messmore, B. W. *J. Phys. Chem. B* **2000**, *104*, 9943.

(14) Stabel, A.; Heinz, R.; Rabe, J. P.; Wegner, G.; De Schryver, F. C.; Corens, D.; Dehaen, W.; Süling, C. *J. Phys. Chem.* **1995**, *99*, 8690.

(15) Loponski, G. P.; Wayner, D. D. M.; Wolkow, R. A. *Nature* **2000**, *406*, 48.

(16) Takami, T.; Ozaki, H.; Kasuga, M.; Tsushiya, T.; Yamazaki, Y.; Fukushi, D.; Ogawa, A.; Uda, M.; Aono, M. *Angew. Chem., Int. Ed.* **1998**, *36*, 2755.

10.1021/la027051p CCC: $25.00
Published on Web 04/05/2003

light-induced polymerization of diacetylene compounds in physisorbed monolayers at the liquid/solid interface with STM.[19] The polymerization product, polydiacetylene, is a π-conjugated linear polymer chain. Conjugated polymers, such as polyacetylene, polythiophene, polypyrrole, and polyaniline, have interesting physical properties including metallic and even superconducting behavior.[23] They find applications in electronic devices such as light-emitting diodes (LEDs), field-effect transistors, and conductive wires.[15,24−27] Therefore, one-dimensional (1D) polydiacetylene nanostructures could be potential parts of molecular electronic nanodevices.

Recently, polydiacetylene chain formation locally induced by an STM tip was reported.[26,27] Aono et al. discussed the formation of conjugated diacetylene polymer chains in monolayer thin films on graphite. They prepared the diacetylene monomer film by the horizontal lifting method. In contrast to the conventional Langmuir−Blodgett (LB) technique, in the horizontal lifting method the substrate is brought parallel to the air/water interface and merely touches the water surface, and the molecules are transferred at relatively low surface pressures.[28] This results in an ordered monolayer structure with the molecules lying parallel to the substrate. Aono et al. succeeded in creating organic nanostructures with a spatial precision of about 1 nm induced by the STM tip, and their results show that STM could be a tool for controlled nanoscale fabrication. However, this control is limited in terms of the direction of the polymerized chains, which is governed by the symmetry of the underlying graphite substrate. In addition, to fabricate 2D nanostructures, other molecular designs are mandatory.

In this paper, we report on the light- and STM-tip-induced polymerization of diacetylene derivatives in monolayers on graphite. We investigated two diacetylene derivatives to compare the molecular organization and its effect on the polymerization, aiming at the formation of 1D and 2D nanostructures. The isophthalic acid derivative (ISA-DIA) contains one side chain with a diacetylene moiety in the middle of the chain (Figure 1). The terephthalic acid derivative (TTA-DIA), which has been designed and synthesized for the purpose of forming 2D linked nanostructures, has two side chains, each one carrying a diacetylene moiety (Figure 1). To investigate the influence of film preparation on the molecular organization and polymerization characteristics, several film preparation conditions were explored.

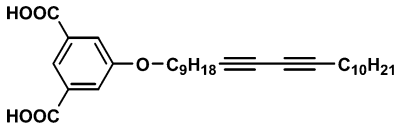

ISA-DIA

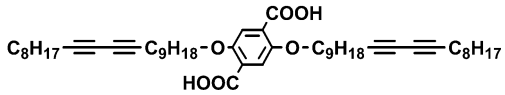

TTA-DIA

Figure 1. Chemical structures of ISA-DIA and TTA-DIA.

2. Experimental Section

2.1. Synthesis of Diacetylene Derivatives. Scheme 1 summarizes the synthetic route to the diacetylene derivatives, 5-(10,12-tricosadiinyloxy) isophthalic acid (ISA-DIA) and 2,5-(10,12-heneicosadiinyloxy) terephthalic acid (TTA-DIA), studied in this work. Both diacetylene derivatives were synthesized as described below briefly.

2.1.1. Synthesis of 5-(10,12-Tricosadiynyloxy)isophthalic Acid (ISA-DIA, 1). *1-Bromo-dodec-1-yne (**3**).*[29] A flask filled with 3.4 g (0.140 mol) of small Mg pieces was dried by heating under high vacuum and flushed with argon. Dry diethyl ether (250 mL) was added, and 15.04 g (10.30 mL, 0.138 mol) of ethylbromide was slowly added to the stirred solution. Once the Mg had completely dissolved, 22.9 g (0.138 mol) of 1-dodecyne was added dropwise. After 3 h, the solution was cooled to −78 °C, and 3.55 mL (11.03 g, 0.138 mol) of bromine was added slowly at a rate which kept the temperature below −70 °C. After the brown color of bromine had disappeared, the reaction was stirred for another 3 h at room temperature. To isolate the product, 100 mL of H_2O and 10 mL of acetic acid were added to the ice-cooled solution. The organic layer was washed twice with a saturated aqueous solution of $NaSO_3$ and H_2O and dried over $MgSO_4$. Evaporation of solvents gave an oily liquid which was purified by vacuum distillation. Yield: 20.3 g (83 mmol), 60%; bp: 79−82 °C (6×10^{-2} mbar). ^{1}H NMR (200 MHz, $CDCl_3$): $\delta = 2.20$ (t, 2H, $J = 7.0$ Hz $-CH_2-\equiv-Br$), 1.65−1.15 (m, 16 H, $-CH_2-$), 0.90 (t, 3H, $J = 6.5$ Hz, $-CH_3$). ^{13}C NMR (50 MHz, $CDCl_3$): $\delta = 80.9$, 68.4, 37.9, 32.4, 30.0, 29.8, 29.6, 29.5, 28.8, 23.1, 20.2, 14.5. FD-MS: $m/z = 245.1$ (M^+).

*10,12-Tricosadiyn-1-ol (**4**).*[30,31] 10-Undecin-1-ol (10.31 g, 0.105 mol) was dissolved in 100 mL of methanol, and a solution of 0.21 g of Cu^ICl and 0.53 g of $NH_2OH{\cdot}HCl$ in 16 mL of aqueous ethylamine (v/v, 1/1) was added. Argon was bubbled through the mixture for 15 min to remove oxygen. A solution of 25.7 g (0.105 mol) of 1-bromo-dodec-1-yne dissolved in 30 mL of methanol was added over 30 min with vigorous stirring, ensuring that the temperature remained constant. If the color of the solution changed to blue, an additional small amount of $NH_2OH{\cdot}HCl$ was added. The reaction was stirred for 3 h at room temperature, and then the solution was diluted with 300 mL of H_2O and extracted with diethyl ether. The combined organic phases were washed with saturated Na_2CO_3 and H_2O and dried with $MgSO_4$. Pure product was obtained by evaporation of the solvent and several recrystallizations from ethyl acetate and heptane. Yield: 18.8 g (56.7 mmol), 54%; colorless solid. ^{1}H NMR (200 MHz, $CDCl_3$): $\delta = 3.65$ (t, 2H, $J = 7$ Hz, $-O-CH_2$), 2.25 (t, 4H, $J = 7$ Hz, $-CH_2-\equiv-\equiv-CH_2-$), 1.65−1.14 (m, 30 H, $-CH_2-$), 0.89 (t, 3H, $J = 6.1$ Hz, $-CH_3$). ^{13}C NMR (75 MHz, DMSO-d_6): $\delta = 68.5$, 65.6, 63.4, 33.2, 32.3, 30.0, 29.9, 29.8, 29.7, 29.5, 29.4, 29.2, 28.7, 26.1, 23.1, 19.6, 14.5. FD-MS: $m/z = 333.0$ (M^+), 664.1 ($2 \times M^+$), 997.2 ($3 \times M^+$), 1329.2 ($4 \times M^+$), 1662.3 ($5 \times M^+$), 1993.2 ($6 \times M^+$).

(17) Heinz, R.; Stabel, A.; Rabe, J. P.; Wegner, G.; De Schryver, F. C.; Corens, D.; Dehaen, W.; Süling, C. *Angew. Chem., Int. Ed.* **1994**, *33*, 2080.
(18) Vanoppen, P.; Grim, P. C. M.; Rucker, M.; De Feyter, S.; Moessner, G.; Valiyaveettil, S.; Müllen, K.; De Schryver, F. C. *J. Phys. Chem.* **1996**, *100*, 19636.
(19) Grim, P. C. M.; De Feyter, S.; Gesquière, A.; Vanoppen, P.; Rucker, M.; Valiyaveettil, S.; Moessner, G.; Müllen, K.; De Schryver, F. C. *Angew. Chem., Int. Ed.* **1997**, *36*, 2601.
(20) Abdel-Mottaleb, M. M. S.; De Feyter, S.; Gesquière, A.; Sieffert, M.; Klapper, M.; Müllen, K.; De Schryver, F. C. *Nano Lett.* **2001**, *1*, 353.
(21) Wegner, G. *Z. Naturforsch., B* **1969**, *24*, 824.
(22) Tieke, B.; Lieser, G.; Wegner, G. *J. Polym. Sci., Polym. Chem. Ed.* **1979**, *17*, 1631.
(23) MacDiarmid, A. G. *Angew. Chem., Int. Ed.* **2001**, *40*, 2581.
(24) Burroughes, J. H.; Bradley, D. D. C.; Brown, A. R.; Marks, R. N.; Mackay, K.; Friend, R. H.; Burns, P. L.; Holmans, A. B. *Nature* **1990**, *347*, 539.
(25) Irie, S.; Isoda, S.; Kobayashi, T.; Ozaki, H.; Mazaki, Y. *Probe Microsc.* **2000**, *2*, 1.
(26) Okawa, Y.; Aono, M. *Nature* **2001**, *409*, 683.
(27) Okawa, Y.; Aono, M. *J. Chem. Phys.* **2001**, *115*, 2317.
(28) Kuroda, R.; Kishi, E.; Yamano, A.; Hatanaka, K.; Matsuda, H.; Eguchi, K.; Nakagiri, T. *J. Vac. Sci. Technol., B* **1991**, *9*, 1180.
(29) *Methoden der organischen Chemie (Houben-Weyl)*, 4th ed.; Georg Thieme Verlag: Stuttgart, 1977; Vol. 5, 2a, S. 931.
(30) Klapper, M. Ph.D. Thesis, University of Mainz, Mainz, Germany, 1990.
(31) Chodkiewicz, W. *Ann. Chim.* (*Paris*) **1957**, *13*, 819, 867.

Scheme 1. Synthesis of 5-(10,12-Tricosadiynyloxy)isophthalic Acid (ISA-DIA, 1) and 2,5-Bis(10,12-henicosadiynyloxy)terephthalic Acid (TTA-DIA, 2)

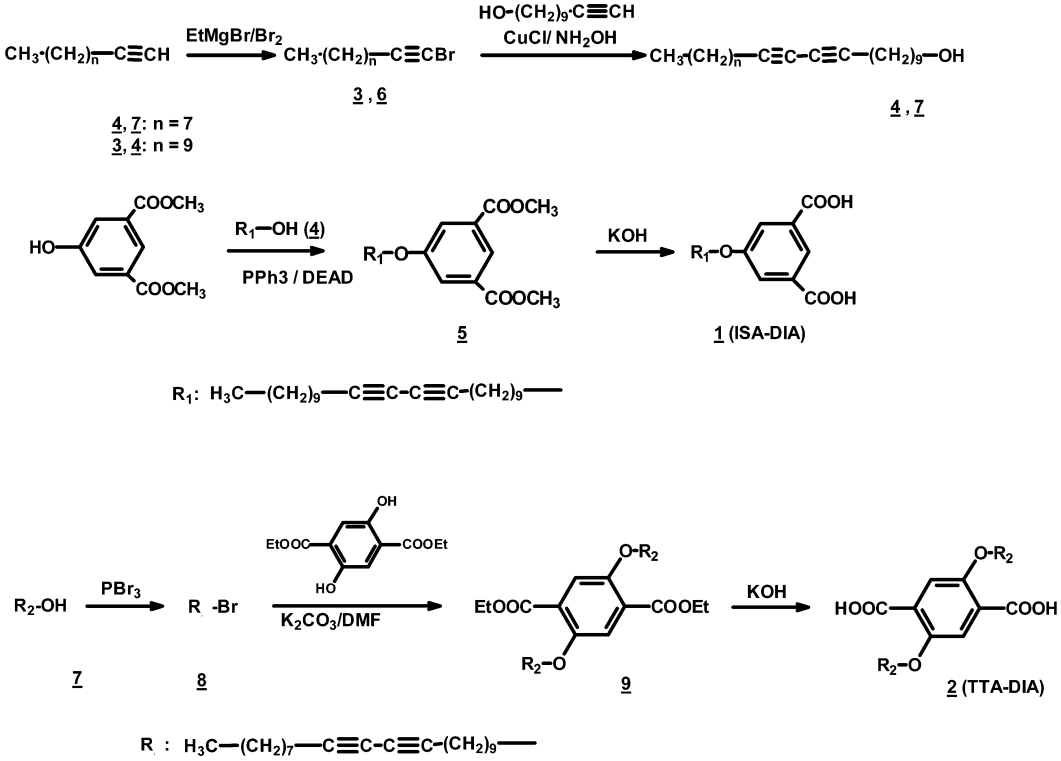

*Dimethyl-5-(10,12-tricosadiynyloxy)isophthalate (**5**).* Dimethyl-5-hydroxyisophthalate (6.13 g, 29.2 mmol) was dissolved in 200 mL of dry diethyl ether under argon. To this solution, 9.72 g (29.2 mmol) of 10,12-tricosadiyn-1-ol and 7.66 g (29.2 mmol) of triphenylphosphine were added. A solution of 5.09 g (29.2 mmol) of azodicarboxylic acid diethylester in 50 mL of diethyl ether was added dropwise at −5 °C. The yellow solution decolored within 15 min, after which the mixture was stirred for 8 h at room temperature. The precipitate (triphenylphosphineoxide) was removed by filtration, the diethyl ether was evaporated, and the colorless solid obtained was purified by recrystallization from methanol. Yield: 10.84 g (20.7 mmol), 71%; mp: 43−44 °C. ^{1}H NMR (200 MHz, $CDCl_3$): δ = 8.26 (s, 1H, ArH), 7.73 (s, 2H, ArH), 4.03 (t, 2H, J = 7.2 Hz, $-O-CH_2$), 3.93 (s, 6H, $COOCH_3$), 2.23 (t, 4H, J = 7 Hz, $-CH_2-\equiv-\equiv-CH_2-$), 1.88−1.73 (m, 2H, $-O-CH_2CH_2-$), 1.57−1.17 (m, 28H, $-CH_2-$), 0.88 (t, 3H, J = 6.4 Hz, $-CH_3$). ^{13}C NMR (50 MHz, $CDCl_3$): δ = 166.9, 159.7, 132.2, 123.2, 120.3, 69.1, 65.7, 52.8, 32.3, 30.0, 29.9, 29.8, 29.7, 29.5, 29.4, 29.3, 29.0, 28.8, 26.4, 23.1, 19.7, 14.5. FD-MS: m/z = 524.1 (M^+), 1084.2 (2 × M^+), 1572.3 (3 × M^+).

*5-(10,12-Tricosadiynyloxy)isophthalic Acid (ISA-DIA, **1**).* The diester **5** (7.07 g, 13.5 mmol) was mixed with ethanol/H_2O (2/1 v/v) and 2.7 g (48 mmol) of KOH and then refluxed for 6 h. By evaporation of the alcohol and acidification with HCl, the acid was precipitated as a colorless solid which was dissolved in diethyl ether. The organic layer was washed with water and dried in the presence of $MgSO_4$. After filtration and evaporation, the acid was obtained as a colorless solid, which was purified by recrystallization from methanol. Yield: 5.36 g (10.8 mmol), 80%; mp: 146 °C. ^{1}H NMR (200 MHz, DMSO-d_6): δ = 8.07 (s, 1H, ArH), 7.63 (s, 2H, ArH), 4.07 (t, 2H, J = 6.1 Hz, $-O-CH_2$), 2.27 (t, 4H, J = 6.8 Hz, $-CH_2-\equiv-\equiv-CH_2$), 1.82−1.63 (m, 2H, $-O-CH_2CH_2-$), 1.52−1.12 (m, 4H, $-CH_2-$), 0.86 (t, 3H, J = 6.4 Hz, $-CH_3$). ^{13}C NMR (50 MHz, DMSO-d_6): δ = 166.7, 159.1, 132.9, 122.4, 119.3, 78.2, 68.4, 65.6, 31.5, 29.1, 28.9, 28.8, 28.6, 28.4, 28.0, 25.6, 22.3, 18.6, 14.2. FD-MS: m/z = 496.5 (M^+), 993.0 (2 × M^+), 1488.1 (3 × M^+), 1985.3 (4 × M^+). Elemental analysis ($C_{31}H_{44}O_5$) calcd (%): C, 74.95; H, 8.93. Found (%): C, 74.55; H, 9.01.

2.1.2. Synthesis of 2,5-(10,12-Henicosadiynyloxy) Terephthalic Acid (TTA-DIA, 2). *1-Bromo-dec-1-yne (**6**).* 1-Bromo-dec-1-yne was obtained according to the procedure described for 1-bromo-dodec-1-yne (**3**). Yield: 9.28 g (0.0427 mol, 31%), colorless oil; bp: 50−55 °C (5 × 10^{-5} mbar). ^{1}H NMR (200 MHz $CDCl_3$, 25 °C): δ = 2.22 (t, 2H, ^3J(H,H) = 7.0 Hz, $-CH_2-\equiv-$Br), 1.65−1.25 (m, 12H, $-CH_2-$), 0.91 (t, 3H, ^3J (H,H) = 7.0 Hz, $-CH_3$). ^{13}C NMR (50 MHz CDCl3, 25 °C): δ = 80.9, 68.4, 37.7, 32.1, 29.6, 29.4, 29.2, 23.1, 20.2, 14.2. FD-MS: m/z = 216.1 (M^+).

*10,12-Henicosadiyn-1-ol (**7**).* 10,12-Henicosadiyn-1-ol was obtained according to the procedure described for 10,12-tricosadiyn-1-ol. Yield: 7.1 g (23 mmol), 55%; colorless powder. ^{1}H NMR (200 MHz, $CDCl_3$, 25 °C): δ = 3.63 (t, 2H, ^3J (H,H) = 6.6 Hz, $-CH_2-OH$), 2.23 (t, 4H, ^3J (H,H) = 6.6 Hz, $-CH_2-\equiv-\equiv-CH_2-$), 1.55−1.26 (m, 26H, $-CH_2-$), 0.87 (t, 3H, ^3J (H,H) = 6.2 Hz, $-CH_3$). ^{13}C NMR (50 MHz, $CDCl_3$, 25 °C): δ = 68.8, 65.8, 65.7, 63.5, 33.2, 32.3, 29.9, 29.8, 29.7 29.5, 29.4, 29.2, 28.8, 26.2, 23.1, 19.6, 14.5. FD-MS: m/z = 305.2 (M^+). Elemental analysis ($C_{21}H_{36}O$) calcd (%): C, 82.83; H, 11.82. Found (%): C, 82.95; H, 12.00.

*10,12-Henicosadiyn-1-bromide (**8**).* Phosphorus tribromide (0.531 g, 0.19 mL, 1.96 mmol) was added dropwise to a solution of 1 g (3.27 mmol) of 8,10-uncosadiyn-1-ol in 30 mL of toluene under argon at 0 °C; then the reaction mixture was stirred for 8 h at room temperature. The solution was diluted with CH_2Cl_2 and washed twice with water. The organic phase was dried over $MgSO_4$, and the solvents were evaporated. The viscous product was purified by column chromatography on silica gel (CH_2Cl_2/petrolether 1:4, R_f = 0.85) to give the product as a colorless oil. Yield: 0.67 g (1.8 mmol), 55%. ^{1}H NMR (200 MHz, $CDCl_3$, 25 °C): δ = 3.40 (t, 2H, ^3J (H,H) = 7.0 Hz, $-CH_2-$Br), 2.24 (t, 4H, ^3J (H,H) = 6.4 Hz, $-CH_2-\equiv-\equiv-CH_2-$), 1.85 (m, 2H, CH_2CH_2Br), 1.51−1.27 (m, 24H, CH_2), 0.88 (t, 3H, ^3J (H,H) = 6.0 Hz, CH_3-CH_2). ^{13}C NMR (50 MHz, $CDCl_3$, 25 °C): δ = 65.3, 65.2, 33.8, 32.8, 31.8, 29.2, 29.1, 29.0, 28.9, 28.8, 28.7, 28.6, 28.3, 28.2, 28.1, 22.6, 19.2, 14.1. FD-MS: m/z = 368.6 (M^+). Elemental analysis ($C_{21}H_{35}$Br) calcd (%): C, 68.65; H, 9.60. Found (%): C, 69.72; H, 9.68.

*Diethyl-2,5-bis(10,12-henicosadiynyloxy)terephthalate (**9**).* Dimethyl-4,6-dihydroxyisophthalate (14.3 mg, 0.056 mmol) and 157 mg (0.412 mmol) of K_2CO_3 were suspended in anhydrous DMF (15 mL) and stirred for 30 min. 8,10-Uncosadiyn-1-bromide (45 mg, 0.122 mmol) in 2 mL of DMF was added, and the solution was stirred for 8 h at 80 °C under argon. Most of the solvent was then removed on the rotary evaporator, and the residue was

dissolved in water and extracted three times with diethyl ether. The organic phase was dried over $MgSO_4$, and the solvent was removed in vacuo. The crude product was purified by column chromatography (petrolether/ethyl acetate 12:1 as eluent, R_f = 0.5). The pure product crystallized on standing to give a colorless solid. Yield: 44 mg (0.053 mmol), 94%. ^{1}H NMR (200 MHz, $CDCl_3$, 25 °C): δ = 7.31 (s, 2H, ArH), 4.33 (q, 4H, ^3J (H,H) = 7.2 Hz, OCH_2CH_3), 3.97 (t, 4H, ^3J (H,H) = 6.2 Hz, $ArOCH_2$), 2.22 (t, 8H, ^3J (H,H) = 6.4 Hz, $-CH_2-\equiv-\equiv-CH_2-$), 1.80−1.74 (m, 4H, OCH_2CH_2), 1.55−1.27 (m, 54H, CH_2, CH_3CH_2O), 0.83 (t, 6H, ^3J (H,H) = 6.4 Hz, CH_3CH_2). ^{13}C NMR (75 MHz, $CDCl_3$, 33 °C): δ = 165.95, 151.73, 124.76, 116.64, 88.88, 69.89, 65.71, 61.26, 31.80, 29.38, 29.29, 29.12, 29.04, 28.84, 28.34, 25.94, 22.82, 19.19, 14.28, 14.06. FD-MS: m/z = 826.6 (M^+). Elemental analysis ($C_{56}H_{82}O_6$) calcd (%): C, 78.40; H, 9.99. Found (%): C, 78.51; H, 10.05.

*2,5-Bis(10,12-henicosadiynyloxy)terephthalic Acid (TTA-DIA, **2**).* Diethyl-2,5-bis(8,10-henicosadiynyloxy) terephthalate (44 mg, 0.053 mmol) was hydrolyzed at 80 °C in a mixture of 17.8 mg (0.32 mmol) of KOH in 3 mL of aqueous ethanol (v/v, 1/1) (TLC control). To isolate the acid, the mixture was extracted with ethyl acetate. After addition of 40 mg (0.047 mmol) of concentrated HCl to the aqueous phase, the product precipitated as a colorless powder. Yield: 40 mg (0.047 mmol, 95%); mp: 178 °C. ^{1}H NMR (300 MHz, DMSO, 25 °C): δ = 7.01 (s, 2H, ArH), 3.88 (t, 4H, ^3J (H,H) = 6.2 Hz, $ArOCH_2$), 2.25 (t, 8H, ^3J (H,H) = 6.6 Hz, $CH_2-\equiv$), 1.63 (m, 4H, $ArOCH_2CH_2$), 1.42−1.23 (m, 48H, CH_2), 0.84 (t, 6H, ^3J (H,H) = 6.8 Hz, CH_3CH_2). ^{13}C NMR (75 MHz, DMSO, 33 °C): δ = 200.33, 166.79, 150.07, 115.70, 77.60, 69.50, 65.04, 30.69, 28.54, 28.34, 28.23, 27.97, 27.86, 27.75, 27.73, 27.36, 27.33, 24.93, 21.48, 17.93, 14.31. EI-MS: m/z = 768.1 (M^+). Elemental analysis ($C_{50}H_{74}O_6$) calcd (%): C, 77.88; H, 9.67. Found (%): C, 77.75; H, 9.80.

2.2. Sample Preparation and Imaging. We examined two different monolayer preparation methods: the horizontal lifting method and drop casting. For the preparation of monolayer films on graphite with the horizontal lifting method, one can take advantage of the amphiphilic properties of ISA-DIA and TTA-DIA. They have both a hydrophobic methylene chain and a hydrophilic carboxylic acid part. Films were prepared in the following way. The diacetylene monomers were dissolved in chloroform (ISA-DIA) or in a chloroform−heptanol mixture in a 9:1 v/v ratio (TTA-DIA). The sample solution was spread onto the Milli-Q water subphase of the LB trough (KSV 5000, KSV Instruments) and compressed to the target surface pressure which was set to approximately 5−7 mN/m and held constant during the deposition. A freshly cleaved highly oriented pyrolytic graphite (HOPG, Advanced Ceramics, ZYB grade) substrate was brought in contact with the air/water interface. Then the HOPG piece was pulled up from the surface, and molecules at the air/water interface were transferred to the substrate surface. Drop-casted films were prepared by applying a drop (<10 μL) of a 0.5 mg/mL solution of ISA-DIA or TTA-DIA in 1-heptanol on a freshly cleaved surface of HOPG. Before imaging, all samples were stored in a desiccator at room temperature in the dark for drying.

STM images were acquired in the variable current mode (constant height) under ambient conditions. In the STM images, white corresponds to the highest and black to the lowest measured scanning tunneling current. STM experiments were performed using a Discoverer scanning tunneling microscope (Topometrix) along with an external pulse/function generator (8111A, Hewlett-Packard), with negative sample bias. Tips were electrochemically etched from a Pt/Ir wire (80%:20%; diameter, 0.2 mm) in an aqueous 2 N KOH/6 N NaCN solution. Experiments were repeated in several sessions using different tips to check for reproducibility and to avoid artifacts. Different settings for the tunneling current and the bias voltage were used, ranging from 0.3 to 0.8 nA and −0.1 to −1.5 V, respectively. During the imaging, little drift of the STM system was detected and care was taken that the same region of the monolayer was imaged during consecutive scans. All STM images contain raw data and are not subjected to any manipulation or imaging processing. A CAMAG universal lamp (wavelength, 254 nm) was used as an UV irradiation source to induce the topochemical polymerization. The lamp was put approximately at a distance of 5 cm above the surface, and the duration of the illumination was between 30 and 45 min.

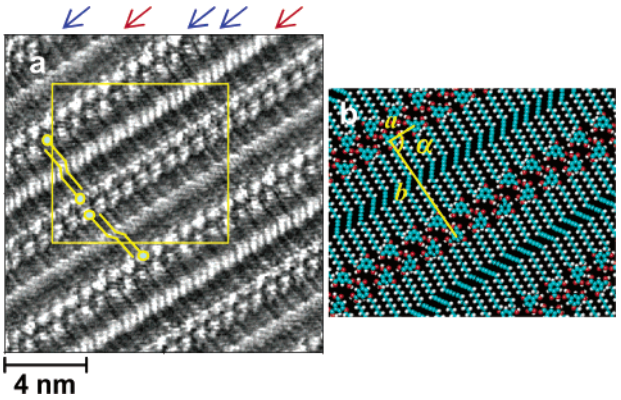

Figure 2. (a) STM image of the ISA-DIA monolayer structure on graphite deposited by the horizontal lifting method. Blue arrows point to the ISA groups, and red arrows indicate the diacetylene moieties in the side chains. Four molecules are schematically drawn in yellow. I_{set} = 0.50 nA, V_{bias} = −0.63 V. (b) Molecular model of the area outlined in (a) and the unit cell parameters.

3. Results and Discussion

3.1. Monolayer Structures of the Diacetylene Derivatives at the Air/Solid Interface. Prior to the polymerization, we examined the monolayer structures of ISA-DIA and TTA-DIA at the air/HOPG interface. Figure 2a shows a typical STM image of the monolayer structure of ISA-DIA prepared by the horizontal lifting method. Molecules form close-packed and well-ordered lamella structures, and individual molecules are clearly resolved with submolecular resolution. The lamella structure is characterized by the isophthalic acid (ISA) group and the diacetylene moiety of the molecules. The ISA groups appear bright and have a circular shape (indicated by the blue arrows), and the diacetylene moieties (indicated by the red arrows) are brighter than the alkyl chains that show a Moiré pattern (a periodic change in contrast of the alkyl chains due to the specific registry with the underlying graphite substrate). The ISA groups of adjacent ISA-DIA molecules point in opposite directions, and the alkyl chains are interdigitated. The orientation of the diacetylene moieties alternates from lamella to lamella. This is different from the monolayers that are formed in the presence of 1-undecanol at the liquid/solid interface.[19] To guide the eye, ISA-DIA molecules have been drawn schematically in Figure 2a. The distance from one ISA group to the next one along the lamella axis is 9.6 ± 0.3 Å. Comparison with the HOPG reference image shows that the alkyl chains of ISA-DIA molecules are lying in the direction of one of the main graphite axes. The unit cell parameters a, b, and α, as indicated in Figure 2b, are a = 9.6 ± 0.3 Å, b = 40.4 ± 0.8 Å, and α = 82 ± 2°. The lamella width is determined to be 34.3 ± 0.3 Å, and the alkyl chains make an angle of 87 ± 2° with respect to the lamella axis.

The monolayer structure of TTA-DIA prepared with the horizontal lifting method is shown in Figure 3a. TTA-DIA forms a well-ordered lamella-like monolayer in which the alkyl chains are two-dimensionally interdigitated and the terephthalic acid (TTA) groups and diacetylene moieties are ordered in rows. TTA groups (indicated with blue arrows) are observed as bright circles, and diacetylene moieties (indicated with red arrows) are located in the center between adjacent rows of TTA groups. In contrast to ISA-DIA, the diacetylene moieties of TTA-DIA are aligned in the same direction throughout a domain. The distance between two neighboring TTA groups within a row (a) and between adjacent rows (b) as part of the unit

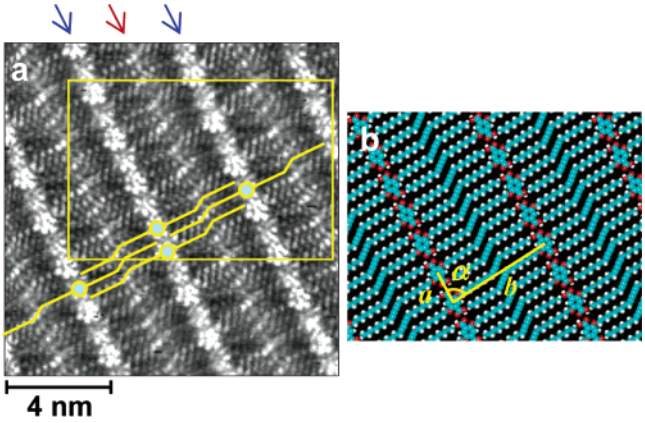

Figure 3. (a) STM image of the TTA-DIA monolayer structure on graphite deposited by the horizontal lifting method. Blue arrows point to the TTA groups, and the red arrow indicates the diacetylene moieties in the side chain. Four molecules are schematically drawn in yellow. $I_{set} = 0.60$ nA, $V_{bias} = -1.10$ V. (b) Molecular model of the area outlined in (a) and the unit cell parameters.

cell is $a = 9.7 \pm 0.3$ Å and $b = 32.5 \pm 0.3$ Å. The angle α measures $86 \pm 3°$. The distance between adjacent rows of TTA groups is determined to be 32.0 ± 0.4 Å, and the alkyl chains make an angle of $85 \pm 2°$ with respect to the row direction. Similar to ISA-DIA monolayers, the alkyl chains are lying parallel to one of the main graphite symmetry axes and the Moiré pattern illustrates the high regularity in the ordering of the alkyl chains.

On the basis of the analysis of the observed monolayer structures, an illustrative molecular model for the molecular arrangement is proposed for both ISA-DIA (Figure 2b) and TTA-DIA (Figure 3b). In their respective three-dimensional (3D) crystals, isophthalic and terephthalic acid derivatives are known to form hydrogen bonding.[32,33] Although the packing in two dimensions does not necessarily reflect the ordering of molecules in solid crystals, the formation of hydrogen bonding is considered to be most likely. In the case of ISA-DIA, neighboring lamellae are expected to interact by hydrogen bonding between the ISA groups.[32] On the other hand, TTA groups are linked by hydrogen bonding along the lamella axis, identical to the situation in three dimensions. This is confirmed by the distance between the TTA groups, which is very similar to the one found in 3D crystals for other terephthalic acid derivatives.[33] Hydrogen bonding assists the formation of close-packed lamella structures and is responsible for the regular alternation of diacetylene orientation. These results illustrate that hydrogen bonding between ISA or TTA groups has a significant influence on the monolayer structure and this noncovalent interaction is ideally suited for controlling the supramolecular ordering in two dimensions.

The films prepared by the horizontal lifting method were transferred at a pressure around 5−7 mN/m on the LB trough. The surface pressure−area (π−A) isotherms of ISA-DIA and TTA-DIA are shown in Figure 4. The π−A isotherm of an isophthalic acid derivative (5-eicosyloxyisophthalic acid) (C20-ISA), which has a methylene chain without a diacetylene moiety, is also shown for comparison. ISA-DIA shows a rapid increase in pressure around 45 Å^2, which is typical for aliphatic acid derivatives. TTA-DIA shows a gradual increase in the pressure starting at ~80 Å^2. This difference in isotherm behavior is caused by the structural difference between ISA-DIA and TTA-DIA. ISA-DIA has only one chain, and it can behave like a simple aliphatic acid. On the basis of the STM observations, the area occupied by one ISA-DIA and TTA-DIA molecule physisorbed on graphite was calculated to be approximately 190 and 310 Å^2, respectively. The films were transferred at a pressure corresponding to a much smaller area per molecule, approximately 30 Å^2 for ISA-DIA and 60 Å^2 for TTA-DIA. From the π−A isotherm of C20-ISA, the molecular area in the tightly packed monolayer on the water surface is estimated to be ~26 Å^2, which corresponds well with the calculated size of the ISA group (~22 Å^2). Therefore, the alkyl chains cannot be in contact with the water surface. Similarly, the alkyl chains of ISA-DIA and TTA-DIA are not lying on the water surface at the surface pressure used for transfer to the graphite substrate. Nevertheless, these conditions resulted in the best monolayer formation. The raised alkyl chains favor the interaction with the nonpolar HOPG substrate, which facilitates the transfer to the substrate. As a matter of fact, the success rate for forming monolayer structures was lower at lower surface pressures (<3 mN/m). However, well-ordered monolayer structures become less frequent at higher surface pressures (>15 mN/m). In addition to well-ordered monolayer structures, unclear patterns, which might be caused by the presence of bilayers, multilayers, or loosely packed monolayers, were observed. Figure 4b shows a typical STM image observed for a TTA-DIA film prepared by the horizontal lifting method at a higher surface pressure. In addition to a monolayer domain in the left and upper right part of the image, unclearly

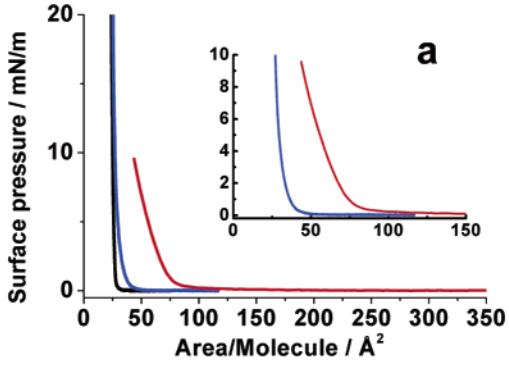

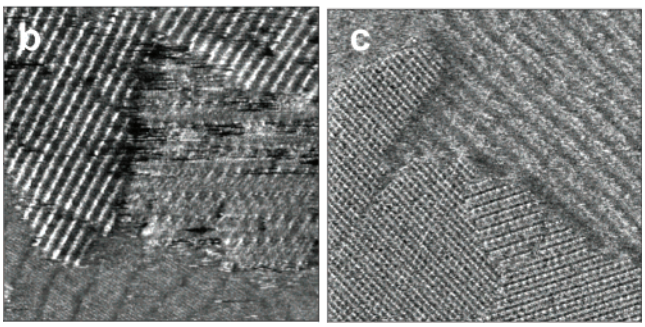

Figure 4. (a) Surface pressure−area (π−A) isotherms of ISA-DIA and TTA-DIA are shown in blue and red, respectively. The π−A isotherm of C20-ISA is shown in black. (b) STM image of a TTA-DIA film prepared by the horizontal lifting method. (c) STM image of a TTA-DIA film prepared by drop casting. The film was prepared from a heptanol solution. In both (b) and (c), in addition to "conventional" monolayer structures, unclearly resolved fuzzy lamellae were observed. The image size is (b) 39.0 × 39.0 nm^2 and (c) 77.2 × 77.2 nm^2.

(32) Valiyaveettil, S.; Müllen, K. *New J. Chem.* **1998**, *22*, 89.
(33) Meiners, C.; Valiyaveettil, S.; Enkelmann, V.; Müllen, K. *J. Mater. Chem.* **1997**, *7*, 2367.

resolved lamellae structures and a fuzzy domain appear at the lower right and bottom part, respectively. The periodicity in the fuzzy pattern differs by a factor of 1.5 from the one in the monolayer structure. This corresponds with neither the width of a TTA-DIA lamella nor the length of heptanol which was used as a solvent. These observations suggest that the nucleation of the molecules on the water surface induced by the surface pressure affects the transfer ratio of the molecules to the substrate and the transfer is followed by a substantial reorganization and reorientation of the molecules on the graphite substrate.

We also examined the monolayer structures of ISA-DIA and TTA-DIA prepared by drop casting. STM images showed monolayer structures similar to those observed for monolayers prepared by the horizontal lifting method, and the difference in unit cell parameters was negligibly small. However, fuzzy patterns similar to those observed for layers prepared by the horizontal lifting method at high surface pressures were frequently observed, both for ISA-DIA and TTA-DIA. Figure 4c shows a typical STM image of a TTA-DIA film prepared by drop casting. Similar to STM images of films prepared by horizontal lifting at high surface pressures, monolayer domains (lower left part) and a fuzzy domain (upper right part) were observed. The periodicity of the fuzzy pattern differs by a factor of 1.5 from the one in the monolayer structure. Due to the lack of resolution, the molecular ordering could not be determined. In view of the inferior quality of the films prepared by drop casting, the polymerization was only attempted in films prepared by the horizontal lifting method.

3.2. Light-Induced Polymerization at the Air/Solid Interface. After the observation and study of monomer diacetylene monolayer structures, light-induced polymerization was attempted. Monolayers of ISA-DIA and TTA-DIA were exposed to UV light. The orientation of the diacetylene units in the supramolecular assembly determines their reactivity in the topochemical polymerization. On the basis of the crystal structures of numerous diacetylene monomers and polymerized diacetylenes, maximal reactivity is expected when the stacking distance between two adjacent diacetylene moieties and the angle between the stacking axis and the diacetylene unit are ~5 Å and ~45°,[34] respectively. The stacking distance and this angle measure 4.8 Å and 50° for ISA-DIA and 4.85 Å and 47° for TTA-DIA, respectively. The stacking distance between two diacetylene moieties is half of the distance between two adjacent ISA or TTA groups. These values indicate that the supramolecular assembly in the monolayer should favor the topochemical polymerization and hence the photoinduced polymerization should be expected upon UV light irradiation.

Figure 5a was obtained after exposing a film of ISA-DIA to UV irradiation. In addition to the monolayer features observed in Figure 2a, a bright line appeared which was never observed before irradiation. The location of the bright line coincides with the diacetylene moieties in nonilluminated films, and hence this bright line is most likely a locally polymerized linear array of diacetylene moieties. In addition to the contrast change, the angle of the alkyl chains with respect to the lamella direction and the lamella width differ significantly between the polymerized array and the nonpolymerized array. As clearly seen in Figure 5b, the alkyl chains of the polydiacetylene make an angle (α_P) of 102 ± 3° with the polydiacetylene backbone, while the alkyl chains are almost perpendicular to the diacetylene array ($\alpha_M = 87 \pm 2°$) for nonpolymerized

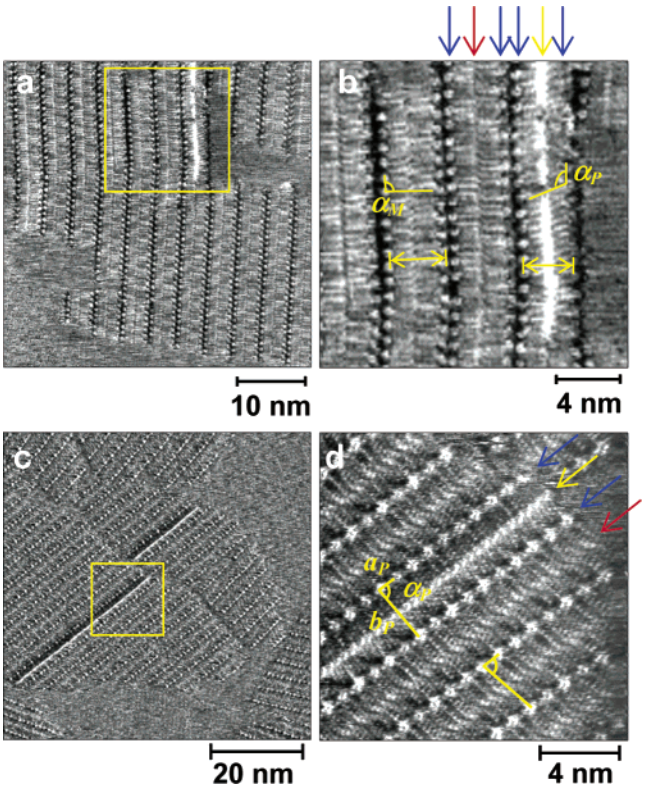

Figure 5. (a) STM image of the ISA-DIA monolayer after 30 min of UV light irradiation. $I_{set} = 0.28$ nA, $V_{bias} = -0.69$ V. (b) Close view of the outlined area in (a). α_P and α_M correspond to the alkyl chain angle against the lamella direction of polymerized and nonpolymerized diacetylene arrays, respectively. Arrows in the figure indicate the lamella width. (c) STM image of the TTA-DIA monolayer after 45 min of UV light irradiation. $I_{set} = 0.45$ nA, $V_{bias} = -0.66$ V. (d) Close view of the outlined area in (c), with a superimposed unit cell of polymerized and nonpolymerized TTA-DIA arrays. Unit cell parameters of the polymerized array (a_P, b_P, α_P) are indicated. Blue, red, and yellow arrows in (b) and (d) point to the ISA and TTA groups, the nonpolymerized diacetylene array, and the polymerized diacetylene array, respectively.

lamellae. The lamella width of the polymerized part decreases by 9% upon polymerization. The ISA group distance along the lamella direction also shows an increase of 4%. These structural changes correspond well with our previous observations for ISA-DIA at the 1-undecanol/graphite interface.[19]

Figure 5c shows the STM image of a monolayer of TTA-DIA after UV irradiation. The bright lines which are considered to be polydiacetylene backbones are observed again. Two polymerized chains are visible in different domains. These chains run along the full length of the domains but are terminated at the domain boundaries. Similar observations are made for ISA-DIA. In addition to the change in contrast, a clear change in the unit cell shape and a small but distinct change in the orientation of the alkyl chains were observed upon polymerization. The unit cell of the polymerized array and the nonpolymerized array are depicted in Figure 5d, which is a close view of the polymerized part in Figure 5c. Interestingly, the interdigitation pattern of the alkyl chains of polymerized TTA-DIA molecules of which the diacetylene units are not involved in the polymerization reaction is not affected. Upon polymerization, the distance between adjacent TTA groups along the array direction increases by 2% and that between neighboring arrays decreases by 6%. The unit cell parameters of the polymerized array are as follows: the distance between nearest neighbor TTA

(34) Enkelmann, V. *Adv. Polym. Sci.* **1984**, *63*, 91.

groups (a_P), the distance between adjacent rows of TTA groups (b_P), and the angle between a_P and b_P (α_P) are $a_P = 9.9 \pm 0.2$ Å, $b_P = 30.6 \pm 0.3$ Å, and $\alpha_P = 89 \pm 1°$, respectively. These structural changes are smaller compared to the polymerization of ISA-DIA.

It is believed that the photoinduced 1,4-topochemical polymerization of diacetylene is initiated by a photochemically generated diradical intermediate, which has unpaired electrons at both ends of the diacetylene moiety. This diradical forms a dimer by 1,4-addition with an adjacent monomer molecule which approaches the diradical by thermally or photochemically induced molecular librations. The diacetylene diradical dimer further reacts with an adjacent diacetylene monomer.[35] An important feature of topochemical polymerization of diacetylene compounds in 3D crystals is that the center axis of the molecular array of the reacting molecules ideally remains fixed during the reaction. Besides that, the polymerization process involves the change in the orientation of the side chains.[34] In analogy with the data revealed by X-ray analysis of 3D crystals, one would also expect the alkyl chains to be tilted after polymerization on the graphite substrate, as shown in Figure 6a. The tilting direction of the alkyl chains should be related to the orientation of diacetylene moieties before polymerization: if one starts with "right-up" monomer, the resulting polymer is expected to be "left-up", and vice versa (Figure 6a). "Right-up" and "left-up" refer to the orientation of the diacetylene unit (for the monomer) and the orientation of the alkyl chains (for the polymer).

As mentioned before, the orientation of the diacetylene groups of ISA-DIA alternates from lamella to lamella. In Figure 5b, the diacetylene groups are considered to have a right-up orientation before polymerization, since the diacetylene groups in the adjacent lamella at the left side have a left-up orientation. Under the assumption that the molecules still lie completely flat on the graphite substrate after the polymerization, the alkyl chains should show the same orientation change as in the model depicted in Figure 6a. In contrast, the opposite side chain orientation is clearly observed in the polymerized part in Figure 5b: the orientation of the alkyl chains is right-up. This is inconsistent with the chain propagation model shown in Figure 6a. One possibility is a local deviation in the regular alternation of the orientation of the diacetylene monomers from lamella to lamella. However, as this polymerized array is observed in a well-ordered monolayer structure, it seems unlikely that a local misalignment of the diacetylene units is responsible for the unexpected orientation of the alkyl chains. In addition, in high-resolution images where the orientation of the diacetylene units could easily be determined, an alternation of the orientation of the diacetylene moieties was always observed.

A disagreement with the polymer chain propagation model, in terms of the alkyl chain orientation, was also observed for the polymerization of TTA-DIA. In the case of TTA-DIA, only a slight change in the angle of the alkyl chains is observed instead of the drastic angle change observed for polymerized ISA-DIA and the chains still fit the lamella structure after polymerization (Figure 5d). These observations imply a certain conformational change upon polymerization. Therefore, we propose a model as shown in Figure 6b in which the alkyl chains are parallel to the graphite surface but the innermost carbon atoms of the alkyl chains adjoining the polydiacetylene backbone and the polydiacetylene backbone itself are raised from the surface. By lifting up the polymer backbone, the alkyl chains can tilt and the model satisfies the experimental observations. Molecular models of polymerized ISA-DIA and TTA-DIA are shown in parts c and e of Figure 6, respectively.

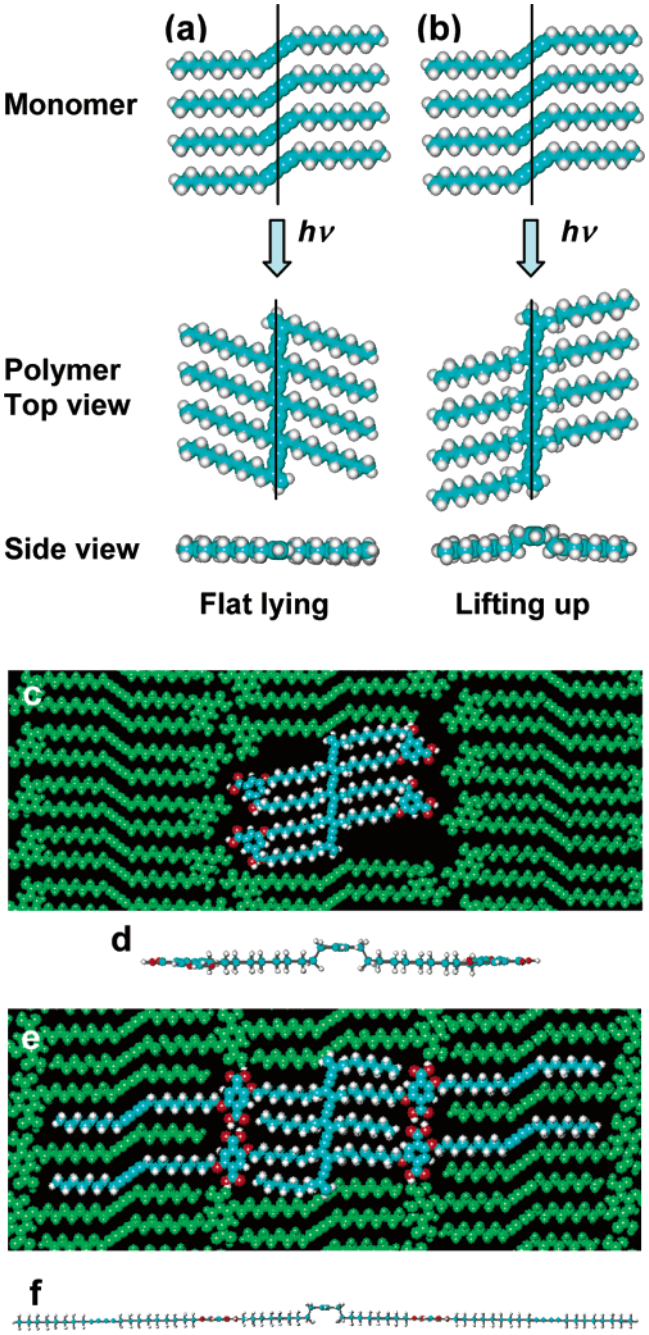

Figure 6. (a) Representation of the topochemical polymerization of model diacetylene compounds. Both the monomer and the polymer lie completely flat on the surface. (b) Tentative molecular model indicating that the polymer backbone is lifted from the substrate upon polymerization. In (a) and (b), "left-up" and "right-up" refer to the orientation of the diacetylene units for monomers and the orientation of the alkyl chains for polymers. (c) Molecular model of polymerized ISA-DIA among nonpolymerized ISA-DIA monomers, which are colored in green. (d) Side view of polymerized ISA-DIA. (e) Molecular model of polymerized TTA-DIA surrounded by TTA-DIA monomers (green). (f) Side view of polymerized TTA-DIA.

Aono et al. also proposed a similar lifted-up structure for the polymer product of 10,12-pentacosadiynoic acid, but for another reason.[26,27] In contrast to our observations,

(35) Neumann, W.; Sixl, H. *Chem. Phys.* **1981**, *58*, 303.

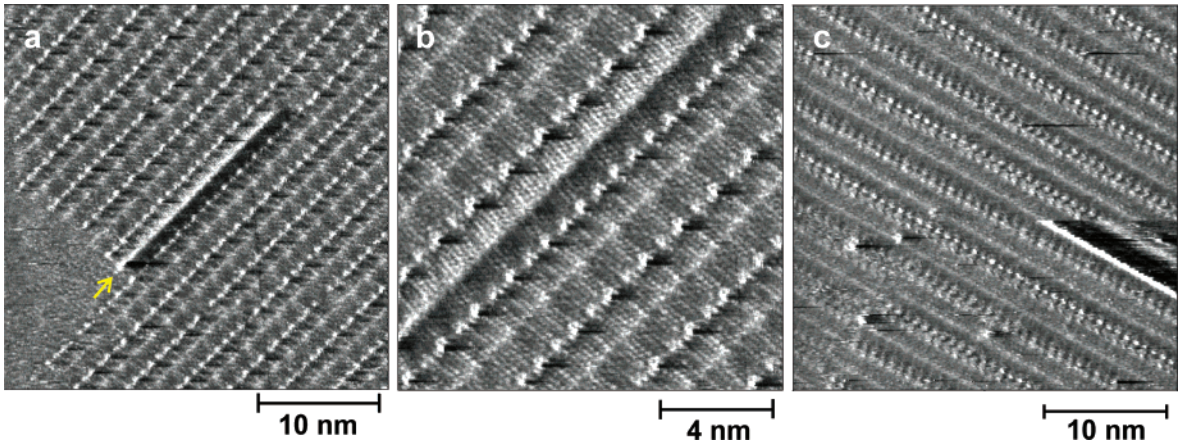

Figure 7. (a) STM image of the TTA-DIA monolayer after application of a single pulse. The pulse was applied at the point indicated in the image. $I_{set} = 0.40$ nA, $V_{bias} = -0.36$ V. The pulse height and pulse width are −3.2 V and 600 ns, respectively. (b) Detailed scan of the polymerized TTA-DIA backbone in (a). (c) STM image of the ISA-DIA monolayer. The bright line in the image which appeared after the application of a bias pulse is a polymerized diacetylene backbone. $I_{set} = 0.40$ nA, $V_{bias} = -0.85$ V. The pulse height and pulse width are −3.2 V and 500 ns, respectively.

they observed identical Moiré patterns of the alkyl chains in the STM images before and after polymerization, which indicates that the alkyl chain orientation in the system is not modulated by the polymerization. The fact that they did not observe a change in the orientation of the alkyl chains implies that some conformational changes must occur upon polymerization: they also concluded that the polymer backbone is lifted up from the substrate.

This model can also successfully explain the brightness of the polydiacetylene backbone in the STM images. According to the model, the polymerized diacetylene backbone is topographically higher than the adjacent side chains. The STM images were recorded in the constant height mode, and a decrease in the distance between the tip and molecule induces a higher tunneling current flow. Hence, the polymerized diacetylene backbone appears brighter in the STM image.

The relative quantity of polymerized ISA-DIA chains per unit area is twice as high compared to that of TTA-DIA, though the light-induced polymerization was carried out under the same experimental conditions. These differences in the polymerization probability can be explained in terms of the spatial flexibility of the molecules in the monolayer structure. The formation of the polydiacetylene backbone involves two important steps. The first is the molecular libration that leads to the 1,4-addition reaction between adjacent diacetylenes in a row. The second is the orientation change of the alkyl side chains. TTA-DIA molecules form a continuous interpenetrating 2D network by interdigitation of the alkyl chains on both sides of the TTA groups and by hydrogen bonding between adjacent TTA groups along the array. In the case of ISA-DIA, interdigitation of the alkyl chains does not lead to a continuous network in two dimensions. Due to this interdigitation, the monolayer structure of TTA-DIA is believed to be more rigid compared to that of ISA-DIA, and hence the polymerization (both initiation and propagation) is expected to be less favored for TTA-DIA.

Furthermore, the extent of polymerization of ISA-DIA in films prepared by the horizontal lifting method is less than at the liquid/solid interface. In the latter environment, polymer chains 100 nm and more in length were observed, which is not the case at the air/solid interface (not shown). The co-deposited solvent molecules and supernatant solvent molecules at the liquid/graphite interface are believed to give rise to a higher mobility or flexibility of the physisorbed molecules, improving the polymerization efficiency.

3.3. Tip-Induced Polymerization: From One Dimension to Two Dimensions. As a next step, we have examined electrochemically induced polymerization by means of an STM tip. Indeed, in addition to the use of UV irradiation, the polymerization of diacetylenes can also be induced by the STM tip. Figure 7a shows the STM image of a polydiacetylene chain of TTA-DIA, of which the formation was initiated by a single bias pulse during the scanning. The pulse was applied at the point indicated in the image, which corresponds to the position of a diacetylene array in the monolayer structure. The height and width of the bias pulse were −3.2 V and 600 ns, respectively. The very bright line is considered to be the polydiacetylene backbone. The molecularly resolved STM image of the polydiacetylene array created in Figure 7a is shown in the close view in Figure 7b. There are no differences in STM contrast and unit cell parameters with the polymerized structure induced by UV irradiation. Therefore, we consider that the tip-induced polymer backbone is also lifted up from the graphite surface. We also examined the tip-induced polymerization of ISA-DIA and succeeded in creating polymerized diacetylene (Figure 7c). The created polymer arrays show the same features as those induced by UV irradiation as in the case of TTA-DIA.

As described above, TTA-DIA can form tightly packed molecularly well-ordered two-dimensional monolayers. Due to the presence of two diacetylene units and the network formation by interdigitation of the alkyl chains, this compound is a potential candidate for the creation of two-dimensional polymers. Figure 8a shows an STM image of a TTA-DIA film prepared by the horizontal lifting method after 30 min of UV irradiation. The bright lines indicate the presence of three polymerized diacetylene rows. The black line, which crosses the image, is a graphite step. After the initial random polymerization induced by UV irradiation, a pulse (height, −3.2 V; width, 500 ns) was applied in the middle of the image, indicated by the white arrow (Figure 8b). A newly created polymerized diacetylene backbone is indicated by the white arrow in Figure 8b. The tip-induced polydiacetylene chain is located next to a UV light induced polymer chain. The upper part of the electrochemically induced polydiacetylene chain is covalently linked, through the terephthalic acid moieties,

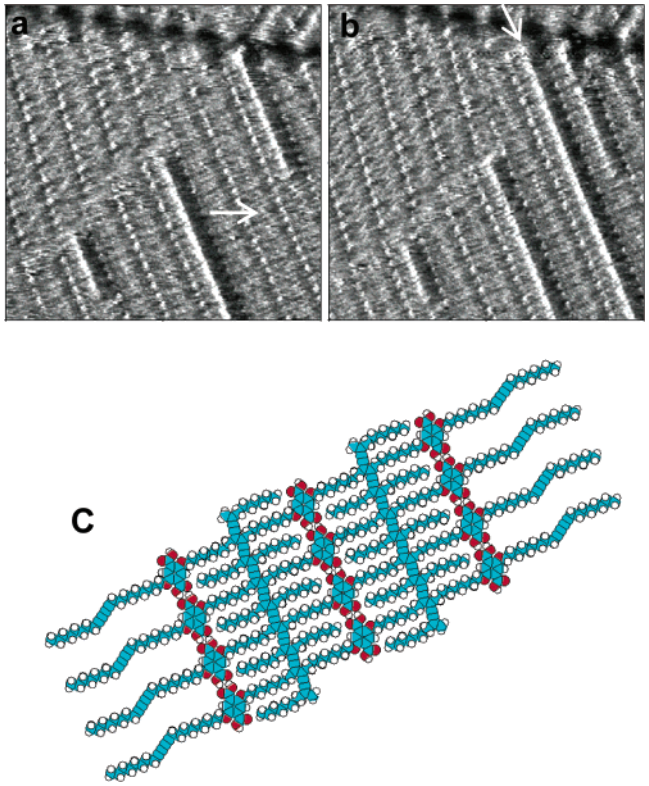

Figure 8. (a) STM image of the TTA-DIA monolayer after 30 min of UV light irradiation. A pulse (height, −3.2 V; width, 500 ns) was applied at the position indicated with a white arrow. (b) STM image of the TTA-DIA monolayer at the same area after application of a single pulse. The white arrow in the image indicates the polydiacetylene backbone created by pulsing. Scanning conditions for both (a) and (b) were the same: I_{set} = 0.40 nA, V_{bias} = −0.40 V. The image size is 27.1 × 27.1 nm^2. (c) Molecular model of a 2D nanostructure formed by the covalent connection of adjacent parallel polydiacetylene chains, as found in the upper part of (b).

with the adjacent polydiacetylene chain. The connection of the 1D polydiacetylene nanostructures leads to the formation of a 2D nanostructure. Figure 8c shows the schematic model of two-dimensionally connected 1D nanostructures of polydiacetylene. Clearly, adjacent rows of polydiacetylene chains are chemically connected and form a 2D nanostructure, in contrast to the formation of isolated 1D polydiacetylene chains.

The tip-induced polydiacetylene chain in Figure 8b propagates in both directions with respect to the location of the pulse. However, we frequently observe the propagation of the polymer chain in only one direction. As stated above, the libration of the diradicals or adjacent monomer diacetylenes is required for the polymerization initiation. The structure of TTA-DIA films is relatively tight, and the libration motion is restricted by the monolayer packing. Furthermore, a small distortion in the packing of the molecules along the lamella axis can induce a misalignment of the diacetylene units which acts as a defect. Therefore, the polymerization in TTA-DIA dry film tends to result in the one-directional polymerization instead of the two-directional polymerization.

Polymerizing adjacent rows of diacetylenes in a controlled fashion is the first step in making a covalently bound two-dimensional network, locally and with nanometer scale resolution, from a well-defined supramolecular architecture. This results in the formation of a 2D polymer with controlled dimensions at the nanometer scale. This illustrates how by careful molecule design in combination with high-resolution manipulation techniques, 2D organic nanostructures can be constructed.

4. Conclusion

We have demonstrated the light- and tip-induced polymerization of compounds with one (ISA-DIA) or two (TTA-DIA) diacetylene functions, at the air/solid interface. Both ISA-DIA and TTA-DIA form well-ordered monolayer structures. The diacetylene-containing compounds can be polymerized upon UV light irradiation, and the polymerization can be induced locally by the STM tip. The polymerized lamellae are not lying flat on the surface: the polymer backbone is probably lifted up from the surface. It was shown for this kind of compound that the polymerization, in contrast to the results of Aono et al.,[26,27] induces a change in the orientation of the alkyl chains, without disturbing the nonpolymerized parts of the monolayer. In addition to the formation of 1D nanostructures, we have demonstrated the possibility for forming 2D nanostructures in a controlled way with nanometer scale precision.

Acknowledgment. The authors thank the DWTC through IUAP-V-03, the EC through the TMR Sisitomas, ESF SMARTON, and the Volkswagenstiftung for financial support. A.M. thanks the Fund for Scientific Research—Flanders for a visiting postdoctoral fellowship. S.D.F. is a postdoctoral fellow of the Fund for Scientific Research—Flanders.

LA027051P